THE JOURNAL OF PHYSICAL CHEMISTRY C

Article

Cite This: J. Phys. Chem. C 2019, 123, 16902−16910

pubs.acs.org/JPCC

Self-Assembly of Alcohols Adsorbed on Graphene

Ronen Zangi*[,†,‡]

[†]POLYMAT & Department of Organic Chemistry I, University of the Basque Country UPV/EHU, Avenida de Tolosa 72, 20018 San Sebastian, Spain

[‡]IKERBASQUE, Basque Foundation for Science, Maria Diaz de Haro 3, 48013 Bilbao, Spain

Supporting Information

ABSTRACT: Self-assembly in two dimensions (2D) can generate structures with no counterparts in three dimensions (3D); therefore, apart from its technological applications, this phenomenon is also theoretically intriguing. We report results from molecular dynamics simulations on the spontaneous crystallization and self-organization of primary and secondary alcohols adsorbed on a graphene sheet. For the 1-alcohol systems, ethanol to 1-decanol, we find the freezing temperatures of the adsorbed alcohols in 2D to be higher than the corresponding values in the 3D bulk. The structures are characterized by linear chains of alcohols held together by a zigzag pattern of hydrogen bonding between neighboring hydroxyl groups, as well as, by dispersive interactions between the alkyl tails. Reminiscent to alkanes in 3D, alcohols with even number of carbons are packed more efficiently than those with odd numbers. Furthermore, alcohols shorter than 1-hexanol exhibit a preference for antiparallel alignment of the dipole moments of neighboring chains, whereas the preferred alignment in longer alcohols is parallel. Although in both cases, herringbone ordering is obtained, in the latter, the 120° kinks are twice as frequent. In contrast to the chain formation of primary alcohols, secondary alcohols form small-sized ring clusters, tetramers for 2-propanol and dimers for 3-pentanol and 4-heptanol. This is a result of steric repulsions between the branched tails that are also manifested in larger distortions of the hydrogen bonds and out-of-plane configurations of the adsorbed alcohols.

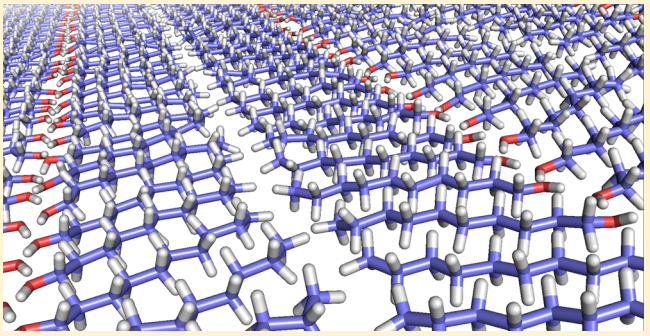

INTRODUCTION

The self-assembled structures of molecules depend on the dimension of the space they occupy. In some cases, the structure in lower dimensions is simply a subspace slice of that in higher dimensions; nevertheless, there are many other cases in which the lower-dimensional structure is unique.[1−4] Aside from the structure, the thermodynamic points marking the transition to an ordered state can also be different.[5−8] For example, the freezing temperature in two dimensions (2D) does not need to be equal to that in three dimensions[9] (3D). This is because the changes in the entropic and enthalpic terms, between the ordered and disordered states, are different in the different dimensions.[10] These arguments are true for purely geometrical considerations, and obviously, also when the interactions of the confining material with the assembled molecules become significant.

The interest in two-dimensional materials is increasing nowadays because of their exploitation in many applications. Two-dimensional organization can be induced by confining the molecules between two surfaces as well as by adsorbing the molecule onto a single surface. In the latter, substantial adsorbent−adsorbate interactions should exist to allow the adsorption and to prevent the fast desorption of the molecules. Amphiphilic molecules possess an inherent tendency to self-assemble, and their interaction with the surface can strongly influence this process.[11] One of the simplest families of amphiphiles is alcohols which are extensively used as solvents in the laboratory and in chemical industries. Moreover, they are also being utilized as materials in many scientific, medical, and commercial applications.

The crystal structures of several *n*-alcohols in 3D resolved by X-ray powder diffraction data are reported in the literature.[12−16] In all cases, a layered structure is formed in which the interlayer interactions alternate between hydrogen bonds (between the hydroxyl groups) and dispersion interactions (between the tails). Thus, the long axis of the molecules is either perpendicular or tilted with respect to the plane of the layers. In the latter, the tilting of the long axes in successive layers can then form a zigzag or parallel pattern. Depending on the temperature, a particular alcohol can exhibit few crystal phases that mainly differ in the orientational order and the tilting degree of the long axis of the molecules, as well as, in trans or gauche bond conformations involving the hydroxyl group atoms. Within each layer, the molecules are arranged in a hexagonal lattice.

In contrast to a crystal, the structure of a liquid is isotropic; thus, beyond the second- or third-neighbor shell structural correlations between the molecules are lost. However, for

Received: May 22, 2019
Revised: June 20, 2019
Published: June 20, 2019

DOI: 10.1021/acs.jpcc.9b04839
J. Phys. Chem. C 2019, 123, 16902−16910

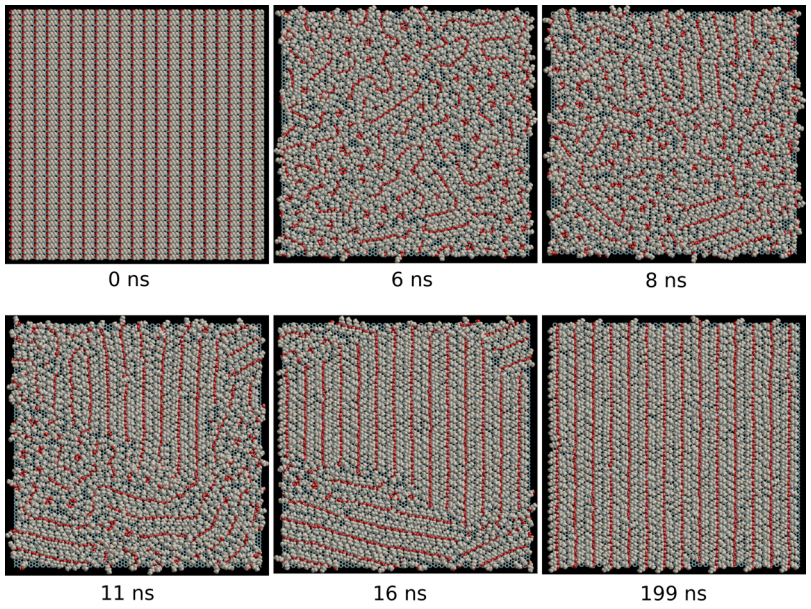

Figure 1. Time evolution of the self-assembly process of 1-butanol on a graphene sheet from a starting configuration of a square lattice. During the first 6 ns, the system was simulated at 200 K and thereafter at 300 K. The snapshot at 199 ns is the last frame of the simulation; nevertheless, a similar configuration is obtained already after 94 ns.

alcohols, a much longer correlation length in the liquid state is believed to exist.[17] Experimental evidence for such long correlations was offered to explain the large anomalous dielectric constants of monohydroxy alcohols,[18] and more directly, a computer simulation study reported that the hydroxyl groups of 1-octanol form long thin chains in the liquid state.[19] In addition, the strong dependency of the dielectric constant on the molecular branching of the tail and on the positioning of the hydroxyl group even led to the suggestion that different structural motifs are formed by different types of alcohols.[20] This argument is also inferred from measurements of the diffusion constants of 1-alcohols and 3-alcohols.[21]

Concerning the behavior of alcohols in reduced dimensions, several studies utilizing the confining cylindrical pores of mesoporous silica materials were performed.[22−25] The results indicate that the temperatures of the freezing/melting and glass transitions are different than those observed for the 3D bulk alcohols. Furthermore, alcohol−water mixtures confined between mica and graphene surfaces exhibited 6 orders of magnitude reduction in the diffusion coefficients relative to the values in bulk.[26] Two-dimensional organization of alcohols can also be generated by adsorption. If the adsorbing material is nonpolar, the strength of the surface−alcohol interaction can be modulated by the length of the alkyl tail without significantly affecting the interactions between the hydroxyl groups. In a series of reports, Morishige and co-workers reported the crystal structure of several *n*-alcohols on graphite by X-ray diffraction measurements.[27−32] The long axis of the alcohol is oriented parallel to the surface, and as the density increases beyond saturation of a monolayer, a second layer is formed with the same orientation[33] (note that in other systems, a density increase beyond saturation can induce a phase transition in which the long axis realigns normal to the surface[34]). In general, the structure exhibits zigzag chains of hydrogen bonds between the hydroxyl groups of the alcohols, whereas the tails in adjacent chains are arranged in a herringbone (chevron) pattern. On contrary to monolayers of alkanes, the positioning of the alcohol molecules is incommensurate with the graphite surface. Similar finding was reported from scanning tunneling microscopy measurements.[35] When determined, the melting temperature of the 2D alcohol crystal on graphite is found to be substantially larger than that in the 3D bulk. For example, 2D ethanol melts at a temperature 50−60 K higher than bulk ethanol.[28,36] It is interesting to point out that for *tert*-butanol, the first layer adsorbed on graphite is a layer of bimolecular thickness.[37] Additionally, in 2-propanol, dimers bound by hydrogen bonding are arranged to give a lamellar structure of the molecules on the surface;[38] however, this determination is not conclusive because of the insensitivity of the diffraction pattern to molecular orientation.

Recently, we investigated the 2D structural organization of methanol.[39] We found extensive formation of long chains of molecules in the liquid state reminiscent of the crystal structure of monolayer alcohols. Upon a decrease in density, these chains transformed into rings. For both motifs, the structural element is held together by hydrogen bonds between the hydroxyl groups, whereas intermotif interactions are of dispersive nature between the tails. Upon a temperature decrease, another transition is observed. In this case, the order−disorder transition is characterized by a low-temperature phase in which the hydrogen bond dipoles of neighboring chains adopt an antiparallel orientation. In this paper, we extend these studies to alcohols with longer alkyl chains adsorbed on a graphene sheet in vacuum.

METHODS

We simulated 12 systems in which a monolayer of alcohol molecules is adsorbed on a graphene sheet. Each system is characterized by alcohol molecules belonging to either primary mono *n*-alcohols (i.e., the series from ethanol to 1-decanol) or symmetric secondary alcohols, 2-propanol, 3-pentanol, and 4-heptanol (see Figure S1). The simulations were performed at the *N*,*V*,*T* ensemble. The graphene sheet (12 264 carbon atoms) oriented parallel to, and occupied entirely, the *xy*-plane

DOI: 10.1021/acs.jpcc.9b04839
J. Phys. Chem. C 2019, 123, 16902−16910

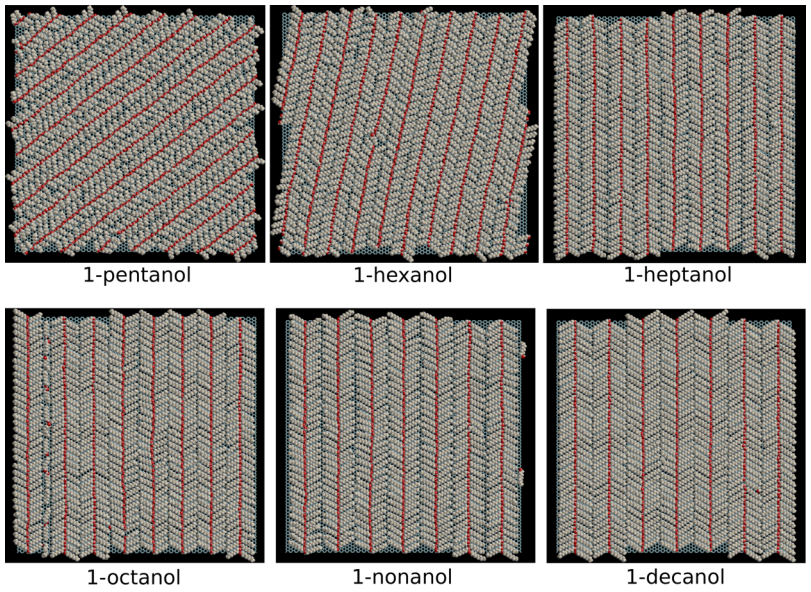

Figure 2. Snapshots of the last configuration of different 1-alcohols adsorbed on a graphene sheet at 300 K.

of the simulation box, has an area of (18.0 × 18.0) 324.0 nm^2. Along the z-axis, the length of the simulation box is 20.0 nm. Thus, except for the graphene and the adsorbed alcohol, the box contains mainly vacuum. Given that all the alcohol molecules are adsorbed, the interaction of the system with its periodic images along the z-axis is effectively eliminated albeit the application of periodic boundary conditions in all directions.

The starting conformation for each alcohol system was a monolayer with a square lattice arrangement (see e.g., Figure 1 at 0 ns). This configuration was then relaxed for 6 ns at a temperature of 200 K. At this low temperature, all alcohols remained adsorbed on the surface even if the structures of the assembly of the molecules were far from equilibrium. Nevertheless, with increasing the temperature, occasional desorption events were observed, especially for molecules whose nearest neighbor interactions were not yet optimized. Therefore, to achieve a full coverage of alcohol molecules on the graphene sheet while the system is searching for the lowest free (Gibbs)-energy structure, we intermittently added or removed molecules to/from the system depending on whether the surface displayed empty regions or molecules evaporated from the monolayer. The addition or removal of molecules was repeated until the monolayer did not accept extra molecules, and no desorption during a time period of at least 60 ns was detected. This yielded a two-dimensional density, $\rho_{2D} = m/A$ (where m is the mass of the molecules and A = 324.0 nm^2 is the area of the graphene sheet), that at full coverage is almost constant for all systems, as shown in the last column of Tables S1 and S2 of the Supporting Information. Initially, we aimed to characterize the adsorption at 300 K for all alcohols; however, for ethanol and 1-propanol, it was difficult to obtain a state without desorption events at this temperature; therefore, for these systems, we simulated the adsorption at a temperature of 250 K. Similarly, 2-propanol also exhibited some degree of desorption at 300 K; thus, the series of the secondary alcohols was studied at 250 K as well. In some cases, to facilitate the escape from a local minimum of the energy surface, the temperature of the system was increased for a period of time and later decreased back to the target temperature. The shortest series of total simulation time was 200 ns for 1-butanol, and the longest was 754 ns for 1-decanol. Simulation time, number of molecules, and temperature of each sub-simulation for the alcohols targeted for adsorption at 300 K are presented in Table S1, and those targeted for adsorption at 250 K are presented in Table S2.

For all simulations, we used the molecular dynamics package GROMACS version 4.6.5[40] with a time step of 0.002 ps. The temperature was maintained by the velocity rescaling thermostat[41] with a coupling time of 0.1 ps. Electrostatic interactions were calculated by the particle mesh Ewald method.[42] The cutoff distance defining the real space was 1.2 nm, and the grid spacing for the reciprocal space was 0.12 nm with quadratic interpolation. Lennard−Jones (LJ) interactions were evaluated by a single cutoff distance of 1.2 nm with long-range dispersion corrections for the energy. Covalent bonds were described by harmonic potentials except those involving hydrogen atoms in which case they were constrained using the LINCS algorithm.[43]

The LJ parameters of the carbon atoms of graphene, σ_{CC} = 0.3851 nm and ϵ_{CC} = 0.4396 kJ/mol, were taken from parameterization of single-walled carbon nanotubes.[44] The carbon−carbon bond length was set to 0.142 nm and C−C−C angle to 120°. During simulations, the positions of the carbon atoms were held fixed and their intrasheet interactions were excluded. The alcohol molecules were described by the mixed-OPLSAA model.[45] This model combines the OPLSAA force-field[46] for the hydroxyl head-group of the alcohol with the L-OPLS force-field[47] for the alkyl chain. Although in general it yields very similar results as the original OPLSAA force-field, it, nonetheless, circumvents the false crystallization of 1-octanol, 1-nonanol, and 1-decanol at room temperature.[45]

RESULTS AND DISCUSSION

Figure 1 exhibits the propagation in time of 1-butanol from the starting conformation to a crystal structure at 300 K. Although in all other simulations, longer relaxation times were applied, similar intermediate stages are observed. In particular, the rapid complete disorder of the starting configuration is followed by the formation of a structure with several crystal

DOI: 10.1021/acs.jpcc.9b04839
J. Phys. Chem. C 2019, 123, 16902−16910

nuclei in different locations with different orientations. Out of this multinuclei nonequilibrium phase, one nucleus grows larger and spreads throughout the entire simulation box. The crystal structure obtained is characterized by infinite (via the periodic boundary conditions of the simulation box) chains of alcohols. Each chain is held by hydrogen bonds, between the hydroxyl groups, with a zigzag pattern (see Figure S2), whereas different chains interact with one another via the dispersion interactions of the tails. As detailed in Table S1, for larger alcohols, we increased the temperature above 300 K at intermediate times to allow faster relaxations, after which we decreased the temperature back to 300 K. Figure 2 presents the last configurations obtained for the series of primary-mono alcohols, from 1-pentanol to 1-decanol. The resulting crystal structures are similar to that obtained for 1-butanol. In most cases, the chains of the alcohols run parallel to the x/y-axis of the simulation box; however, they are slightly tilted in 1-hexanol and strongly tilted, by about 45°, in 1-pentanol. Although the exact reason for this behavior is not clear to us, it might be related to the fact that the average density of the atoms along the axis perpendicular to the hydrogen bond chains is larger than that along the parallel axis. Note that for 1-octanol and 1-nonanol, the system accepts individual molecules to fill-in gaps within the assembly which are not in line with the crystal structure (Figure 2).

Figure 2 implies that the freezing temperatures of the two-dimensional alcohols, from 1-butanol to 1-decanol, on graphene are above 300 K. Experimental studies showed that systems in which the alcohols only partially cover the graphite surface lead to a lower melting temperature relative to a complete coverage. Taken this issue into consideration, we note that the melting of 2D *n*-hexanol and *n*-heptanol was determined to be 284 and 294 K, respectively.[32] Thus, obviously, for these alcohols, there is at least a slight overestimation of the melting temperature and we anticipate a systematic overestimation for the entire series. Note that for bulk alcohols, the mixed-OPLSAA force-field slightly *underestimates* the freezing temperature for 1-octanol, 1-nonanol, and 1-decanol.[45] One plausible explanation for the higher 2D melting temperatures observed (beyond inaccuracies of the force-fields used) is that the positions of the atoms of the graphene sheet were fixed during the simulations and were not allowed to vibrate. Furthermore, it is worth mentioning that for all of the primary-mono alcohols, the adsorbed alcohols formed only a monolayer in which the density profiles normal to the graphene sheets are unimodal (Figure S3).

The hydroxyl group plays an important role in the stability of the chain structure by forming, ideally, two hydrogen bonds, one with each of the two neighboring alcohols of the same chain. Therefore, the conformation involving this hydroxyl group affects the structure of the monolayer. Using vibrational spectroscopy and ab initio molecular orbital calculations, it was determined that 1-butanol in the solid state adopts two conformations for the three dihedral bond axes of the molecule, $CH_3-CH_2-CH_2-CH_2-O-H$.[48] The first is the all-trans, TTt, conformation (T or t denotes trans), and the other is the TTg conformer in which the dihedral angle involving the hydrogen atom of the hydroxyl group is in a gauche (g) conformation. We analyzed the distribution of the two dihedral angles involving the hydroxyl group in Figure 3 and found that for all alcohols considered, both dihedral angles are in a trans conformation (this is also easily visible from the snapshot presented in this figure). Note that for the CH_2-CH_2-O dihedral angle, there is a negligible population in a gauche conformation which decreases for alcohols with longer tails (in fact, for 1-decanol and 1-nonanol, the gauche conformation does not exist).

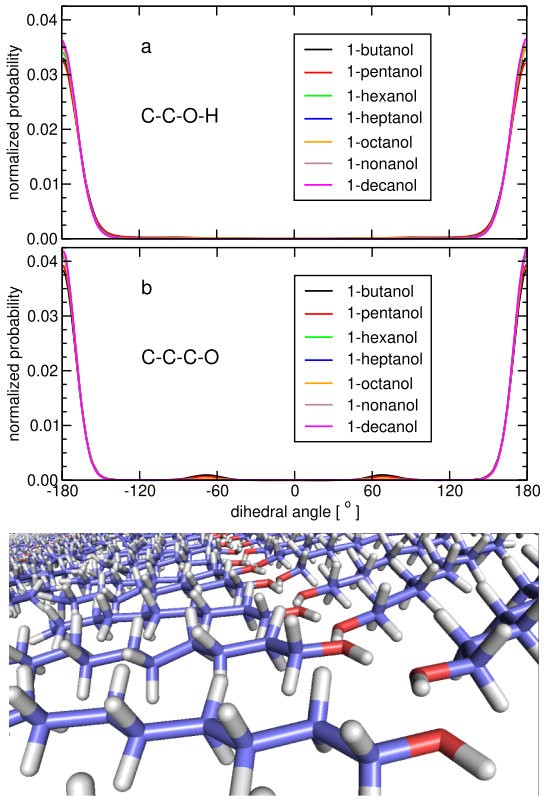

Figure 3. Normalized distributions of (a) C−C−O−H and (b) C−C−C−O dihedral angles of alcohol monolayers crystallized on graphene. Values of ±180° indicate a trans conformation. The lower panel displays an instantaneous configuration of 1-decanol in which the trans conformations of these angles are clearly identified.

As mentioned in the introduction, several studies found that whereas the assembly of *n*-alkanes commensurates with the graphite surface, the organization of 2D alcohols is not. The explanation for this is probably because in alcohols, the adsorbate−adsorbate interactions become significant relative to the interactions of the adsorbate with the surface. In Figure S4, we plot the radial distribution function between the carbon atoms of the alcohols and the carbon atoms of the graphene sheet. A distribution with a flat horizontal line at a value of 1 means a complete random positioning of the alcohols relative to the surface. The results indicate that the distribution is predominantly random. For 1-pentanol and 1-hexanol, the correlations with the surface atoms are completely random; nonetheless, for several alcohols, especially for 1-decanol and 1-butanol, there are small (note the magnitude of the y-axis) correlations expressed by the peak around 0.125 nm. This location, equals $\sin(60°)$ times the C−C bond length in graphene, corresponds to a zigzag alignment which was shown to be the energetically most favorable alignment for alkanes.[35] It is interesting to mention that 1-pentanol and 1-hexanol are the systems in which the chains of the alcohols do not run parallel to the x/y-axis of the simulation box and this might affect the lack of the small preferential alignment. For these two alcohols, it is difficult to detect a penalty in the energy between the alcohol molecules and the surface as the curve in

DOI: 10.1021/acs.jpcc.9b04839
J. Phys. Chem. C 2019, 123, 16902−16910

Figure 4a is essentially linear. In contrast, the interaction energies between the alcohol molecules are not linear but

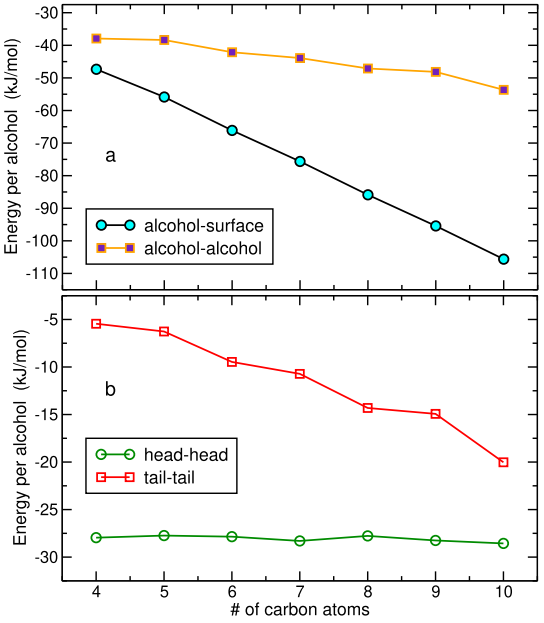

Figure 4. (a) Interaction energy between the alcohol molecules and the graphene surface along with the alcohol–alcohol energy. In the latter, all bonded and 1–4 interactions, as well as nonbonded interactions within the same molecule, are excluded. (b) Decomposition of the interaction between the alcohols to tail–tail and head–head components. The head is defined as the polar $-CH_2OH$ group, whereas the tail is the remaining alkyl moiety of the molecule. The head–tail component, which is not shown, is almost constant for all alcohols ranging from 4.4 to 5.1 kJ/mol. The curves are plotted as a function of the 1-alcohol series from 1-butanol (4 carbon atoms) to 1-decanol (10 carbon atoms). All values are divided by the number of alcohol molecules in the simulation box.

exhibit the well-known even–odd effect of alkanes in bulk crystals.[49] The average alcohol–alcohol energy is more attractive for alcohols with even number of carbon atoms compared to those with odd number. This is shown clearly to originate from the tail–tail interactions, whereas the head–head interactions, dominated by two hydrogen bonds, are constant (Figure 4b). In Figure 5, we display two snapshots showing the packing of the alcohols tails of one chain against an adjacent chain for 1-heptanol and 1-octanol. The figure demonstrates that in 1-octanol, the tails can be packed more efficiently compared to the packing in 1-heptanol. This is also

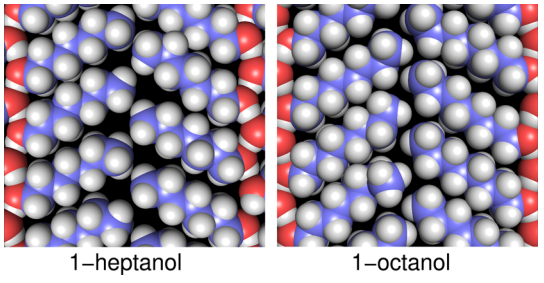

Figure 5. Snapshots taken from Figure 2 showing the packing of the alcohol tails between two different chains for 1-heptanol and 1-octanol. Alcohols with even number of carbon atoms are packed tighter than alcohols with odd carbon atoms.

the case for all other even–odd alcohol pairs; thus, the effect is not only unique to crystal structures in 3D but also exists in 2D alcohol structures.

Because for ethanol and 1-propanol systems, it was difficult to obtain a state without desorption events at 300 K, we simulated these systems at 250 K. The resulting structures are shown in the upper panel of Figure 6. In general, the

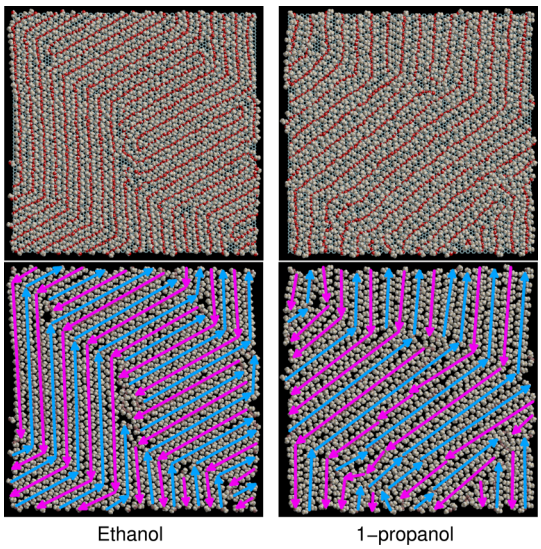

Figure 6. Upper panel: Snapshots of the last configuration of ethanol and 1-propanol adsorbed on graphene at 250 K. Lower panel: Same configurations but with arrows, placed on top of the hydrogen-bonded chains, pointing in the direction of donor-H–acceptor hydrogen-bond dipoles. Arrows colored in cyan and magenta denote hydrogen-bond directions pointing up and down, respectively. In the lower panel, the stick representation of the graphene sheet is not shown.

structures, albeit less ordered, are similar to the structures obtained for the longer alcohols shown above; nevertheless, the chains of the molecules display kinks with an angle of approximately 120°. The magnitude of the fluctuations of the molecules positioning relative to a perfect order suggests that the simulation temperature (250 K) is around the freezing temperature, which for ethanol was determined experimentally[28] to be 215 K.

As shown in Figure 3, when the hydroxyl groups form the zigzag chain of alcohols, the dipole moments of the –OH covalent bonds (or alternatively, the dipole moments of the hydrogen bonds themselves) within the chain, ideally, all point in the same direction. Then, the dipole moments of neighboring chains can either align parallel or antiparallel with respect to the tagged chain. Recently, we showed that below a critical temperature, 2D methanol undergoes order–disorder transition in which the dipole moment alignment of neighboring chains changes from random to antiparallel.[39] In the low-temperature phase, the dipole moments on adjacent chains can interact favorably, if aligned antiparallel, at the expense of entropy. Obviously, the magnitude of this interaction decreases with the distance between the neighboring chains of dipoles, which is directly proportional to the length of the tails. It is therefore not clear, what is the critical value of the alcohol's tail length above which this effect will cease to exist. In the lower panel of Figure 6, we mark the directions of the dipole moment for both, ethanol and 1-propanol, systems. Dipole moments pointing up (or up-right)

DOI: 10.1021/acs.jpcc.9b04839
J. Phys. Chem. C 2019, 123, 16902–16910

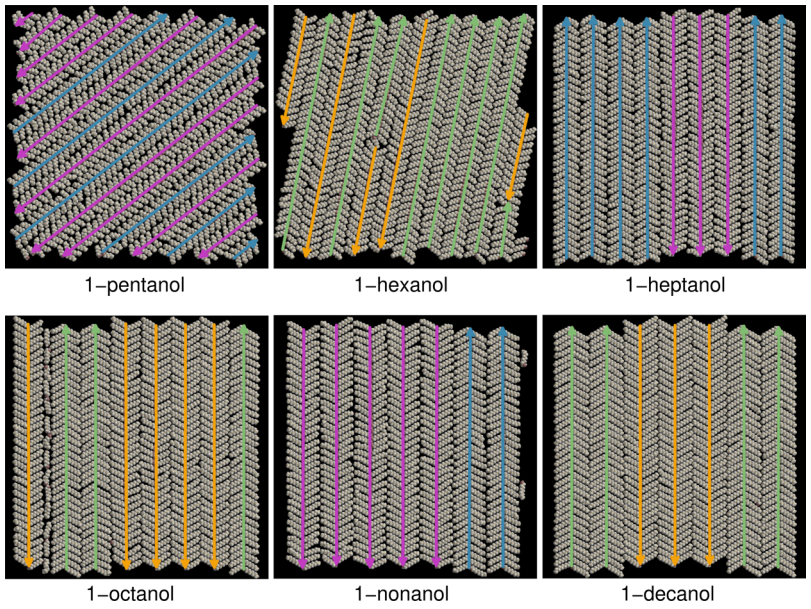

Figure 7. Snapshots shown in Figure 2 but with arrows, placed on top of the hydrogen-bonded chains, pointing in the direction of donor-H–acceptor hydrogen-bond dipoles. Arrows colored in cyan/green and magenta/orange denote hydrogen-bond directions pointing up and down, respectively.

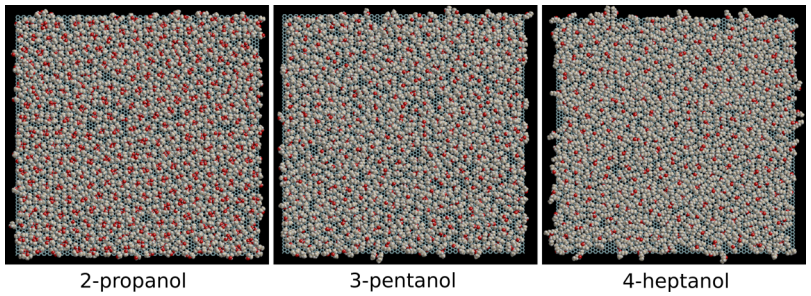

Figure 8. Snapshots of the last configuration of three symmetric secondary alcohols (2-propanol, 3-pentanol, and 4-heptanol) adsorbed on graphene at 250 K.

and down (or down-left) are denoted by different colors. Except of one incident in ethanol and three incidents in 1-propanol, all adjacent chains align antiparallel to one another.

We extend this dipole moment alignment analysis to the crystal structures of the longer alcohols. In Figures S5 and 7, we show the structures of 1-butanol to 1-decanol with arrows on top of the hydrogen-bonded chains (pointing in the direction of donor-H–acceptor hydrogen-bond dipoles). For 1-butanol, there are 10 alignments out of 14 which are antiparallel. This preference for antiparallel interactions is also evident for 1-pentanol. In contrast, for long alcohols, 1-heptanol to 1-decanol, parallel alignment of the chains dipole is preferred. The 1-hexanol system seems to be the transition point in which the population of parallel and antiparallel alignment is, approximately, equal. Thus, the distance of approximately 12 carbon atoms marks the point for which the enthalpic gain of aligning the dipoles of the chains antiparallel is overcompensated by other effects.

One may wonder, why would a system prefers a parallel dipole moment alignment over a random one given there is some entropic benefit for the latter? Note that in the case of a parallel alignment of the dipole moments, the tails of the molecules on different chains are orientated at an angle of 120° (hereafter referred to as TT_120), whereas for antiparallel dipole alignment, the tails on different chains are orientated at 180° (TT_180). Both tail–tail packings are shown on the left panel of Figure S6. On contrary to the even–odd effect observed above, here, we could not attribute the preference for the TT_120 pattern, exhibited by the larger alcohols, to an increase in packing efficiency. We calculate the distribution of the distance between a methyl group on one chain of alcohols to the two-closest methyl groups on an adjacent chain of alcohols and plot them separately for the TT_120 and TT_180 alignments. The results are shown on the right panel of Figure S6. The distributions are unimodal with a peak at 0.41 nm, as expected from the van der Waals exclusion volume of a methyl group. There are no obvious significant differences between the TT_120 and T_180 curves albeit the narrower shape of the former, and at this point, it is not clear to us the origin of the thermodynamics stability of the TT_120 pattern (or alternatively, the parallel dipole alignment of the chains) exhibited by 1-heptanol to 1-decanol.

We also simulated secondary alcohols. To avoid addressing issues arising from stereoisomers, we chose the symmetric secondary alcohols, 2-propanol, 3-pentanol, and 4-heptanol. The last configurations of these secondary alcohols adsorbed on graphene at 250 K are shown in Figure 8. Contrasting the linear chain formation displayed by the 1-alcohol series, here,

DOI: 10.1021/acs.jpcc.9b04839
J. Phys. Chem. C 2019, 123, 16902–16910

the alcohols are assembled into small clusters of rings. This is likely a consequence of steric repulsion between neighboring molecules. The distribution of the size of these rings is sharply peaked at four for 2-propanol; however, it exhibits a broader curve around a value of two for 3-pentanol and 4-heptanol (see Figure 9a). Thus, when confined to 2D, 2-propanol displays

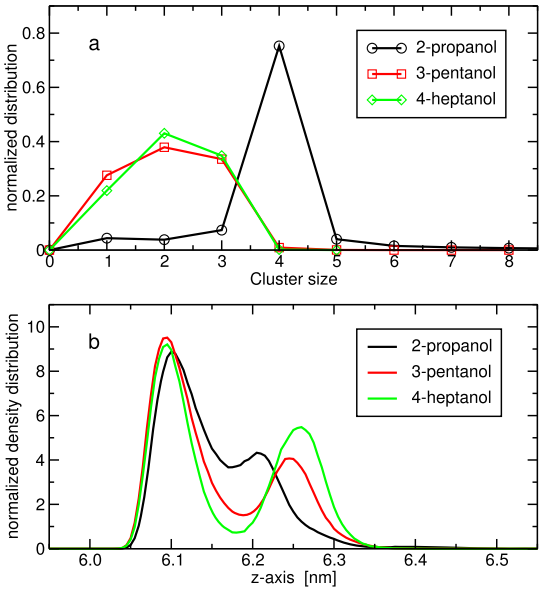

Figure 9. Normalized distributions of (a) size of the ring clusters and (b) density of the oxygen atoms along the normal to the graphene axis (the graphene atoms are located at z = 5.75 nm) for 2D secondary alcohols. In (a), the rings were determined by a distance cutoff of 0.35 nm between the oxygens of different alcohols.

high propensity to form tetramers, which is not in agreement with a report based on X-ray diffraction data,[38] whereas 3-pentanol and 4-heptanol prefer to assemble into dimers. We conjecture that the reason for the different behaviors is because for larger alcohols, the steric repulsion is augmented which prevents the assembly of four molecules to a ring. This steric repulsion affects also the out-of-plane ordering of the alcohols. As mentioned above, the density profiles of the 1-alcohol series are all unimodal (Figure S3); however, for the secondary alcohols studied, the distributions are bimodal with a substantial out-of-plane component. This is shown in Figure 9b for the density profiles of the oxygen atoms. Nonetheless, similar bimodal distributions are obtained for the density of the carbon atoms (graph not shown). The figure indicates that the bimodal character of the density profile increases in magnitude (height and distance from the surface of the second peak) with the length of the alcohol. Note that the organization of the different clusters is not well ordered as in a crystal.

The main reason that the brunched tails of the secondary alcohols inhibits the formation of chains is because the interactions between the hydroxyl groups would not permit hydrogen bondings with an acceptable geometry. In Figure 10, we present the hydrogen-donor−acceptor angle for 1-propanol (forming linear chains as shown in Figure 6) and 2-propanol (forming mostly tetramers rings as shown in Figure 8) adsorbed on graphene at 250 K. In these figures, we included only interactions in which the hydrogen-acceptor distance was smaller than a cutoff value of 2.5 Å. Although there are more distortions from the ideal linear geometry (0°) for 2-propanol,

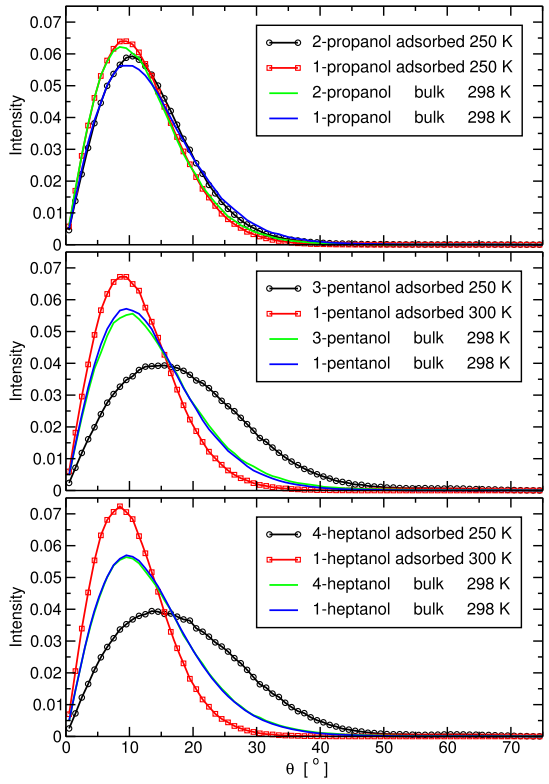

Figure 10. Hydrogen-bond angle (hydrogen-donor−acceptor) distributions of primary and secondary alcohols (propanol, pentanol, and heptanol) adsorbed on a graphene sheet. The corresponding distribution in bulk at 298 K (taken from previous simulations[45]) is shown as well for comparison. We applied a hydrogen-acceptor distance cutoff of 0.25 nm to identify potential hydrogen-bond interactions.

the difference is very small. These distributions are then compared with those obtained by these two alcohols in 3D bulk at 298 K (simulations taken from our previous study[45]). Also here, the differences are small, although quantitative comparison is not possible because of the different temperatures. The smaller distortions of hydrogen bonds observed in bulk 2-propanol compared with those in bulk 1-propanol are likely because the melting temperature of the former is 37 K higher. We performed similar analyses for pentanol and heptanol (Figure 10). On contrary to the propanol case, here, the secondary alcohols, 3-pentanol and 4-heptanol, exhibit large hydrogen-bond distortions compared to the corresponding 1-alcohol even when the latter is simulated at higher temperature of 300 K. These magnitudes of distortions are the reason that 3-pentanol and 4-heptanol form small-sized clusters, that is, dimers, compared to the tetramer rings of 2-propanol. For the bulk alcohols (primary and secondary), the distortion of hydrogen bonds is larger than that for the adsorbed 1-alcohol but smaller than those for adsorbed secondary alcohol.

To quantify the change in the ability to form hydrogen bonds between 2D and 3D assemblies, we calculate in Table 1 the average number of hydrogen bonds an alcohol molecules forms with its neighbors in the different systems. To this end, an angle cutoff (AC) for counting hydrogen bonds has to be determined. On the basis of the shape of the hydrogen-donor−acceptor angle curve, we chose ACs ranging from 25° (for the sharply-peaked distributions) to 40° (for the broadest

DOI: 10.1021/acs.jpcc.9b04839
J. Phys. Chem. C 2019, 123, 16902−16910

Table 1. Average Number of Hydrogen Bonds of an Alcohol Molecule Form with Its Neighboring Alcohols in the 2D (Adsorbed) Assembly[a]

	T [K]	AC	$\langle HB \rangle_{adsorbed}$	$\langle HB \rangle_{bulk298}$
2-propanol	250	30°	1.80	1.78
3-pentanol	250	40°	1.14	1.47
4-heptanol	250	40°	1.20	1.56
1-propanol	250	30°	1.92	1.68
1-pentanol	300	25°	1.92	1.72
1-heptanol	300	25°	1.95	1.72

[a]Hydrogen bonds were determined by a hydrogen-acceptor distance cutoff of 0.25 nm and an AC whose value (determined from the distributions shown in Figure 10) is indicated in the third column. We also display the corresponding values found in bulk at 298 K (calculated from simulations reported previously[45] using an AC of 30°). For all cases, the error is estimated to be equal or less than 0.01.

distributions), enabling to capture each distribution almost entirely. The number of hydrogen bonds of 2-propanol adsorbed on a graphene sheet is slightly smaller than that for 1-propanol. For the larger alcohols, pentanol and heptanol, this reduced ability of the secondary alcohol to form hydrogen bonds in 2D is much larger. For primary alcohols, the effect of confinement to 2D, relative to bulk 3D, is to increase the number of hydrogen bonds and this is one of the reasons for the increase in their melting temperatures. In contrast, secondary alcohols experience a decrease in the ability to form hydrogen bonds in 2D relative to 3D.

CONCLUSIONS

In this paper, we investigated self-assembled monolayers of primary and secondary *n*-alcohols adsorbed on a graphene sheet in vacuum. For the 1-alcohols series, we found that two-dimensional adsorption increases significantly the freezing temperature relative to that in three-dimensional bulk. In particular, utilizing the mixed-OPLSAA force-field, the alcohols from 1-butanol to 1-decanol spontaneously crystallized at 300 K within a time scale of several hundred nanoseconds. Ethanol and 1-propanol displayed crystallization at 250 K. All 2D crystals of the 1-alcohol series exhibited several common features. The main structural motif was a chain of alcohols with a zigzag pattern of hydrogen bondings, in which the dihedral angles involving the hydroxyl groups were in a trans conformation. Adjacent chains interacted with each other via the terminal part of the alcohol's tails, and only weak commensuration with the surface is detected for several systems. The well-known even−odd effect found in bulk alkanes is also observed for alcohols in 2D. That means, alcohol tails with even numbers of carbon atoms are packed more efficiently, and thereby better stabilized enthalpically, than alcohols with odd carbons. Furthermore, the structure of alcohols smaller than 1-hexanol exhibited preference for an antiparallel ordering of the dipole moments of neighboring chains. For short alcohols, this is energetically beneficial because of dipole−dipole interactions. With this alignment of the hydroxyl groups, the tails between alcohols on neighboring chains interact at an angle of 180°. In contrast, for larger alcohols, the ordering of the dipole moments of neighboring chains is parallel and the tail−tail interactions are at an angle of 120°. The origin of the stability of this configuration requires further investigations.

For the secondary alcohols, simulations at 250 K did not result in the formation of chains but in assemblies into ring clusters. The most probable cluster size is four (tetramer) for 2-propanol and two (dimer) for 3-pentanol and 4-heptanol. Steric repulsion is likely the reason for the tendency to form ring clusters instead of chains and for the reduction in cluster size (from four to two) of the larger alcohols. This steric repulsion is also expressed in an increase of the out-of-plane configuration of the monolayer with the alcohol size, as well as, in the distortion of hydrogen bonds between the hydroxyl groups. Except for 2-propanol, the systems of 3-pentanol and 4-heptanol displayed significant distortions of hydrogen bondings compared to the corresponding adsorbed 1-alcohols, as well as to the 3D bulk.

ASSOCIATED CONTENT

Supporting Information

The Supporting Information is available free of charge on the ACS Publications website at DOI: 10.1021/acs.jpcc.9b04839.

Alcohol models, details of the simulations setups, demonstration of the zigzag pattern of the hydrogen bonds, density profiles normal to the graphene plane, correlation between the positions of the alcohols and surface atoms, alignments of the hydrogen-bond dipoles in 1-butanol 2D crystal, and examples of the two different types of interactions between the alcohol tails of adjacent chains (PDF)

AUTHOR INFORMATION

Corresponding Author

*E-mail: r.zangi@ikerbasque.org.

ORCID

Ronen Zangi: 0000-0001-5332-885X

Notes

The author declares no competing financial interest.

ACKNOWLEDGMENTS

This work was supported by a grant from the ministry of economy and competitiveness of the Spanish government, reference number CTQ2016-80886-R. We would like to thank the technical and human support of the computer cluster provided by IZO-SGI SGIker of UPV/EHU and European funding (ERDF and ESF).

REFERENCES

(1) Koga, K.; Zeng, X. C.; Tanaka, H. Freezing of Confined Water: A Bilayer Ice Phase in Hydrophobic Nanopores. *Phys. Rev. Lett.* **1997**, *79*, 5262−5265.

(2) Zangi, R.; Mark, A. E. Monolayer Ice. *Phys. Rev. Lett.* **2003**, *91*, 025502.

(3) Takaiwa, D.; Hatano, I.; Koga, K.; Tanaka, H. Phase Diagram of Water in Carbon Nanotubes. *Proc. Natl. Acad. Sci. U.S.A.* **2008**, *105*, 39−43.

(4) Algara-Siller, G.; Lehtinen, O.; Wang, F. C.; Nair, R. R.; Kaiser, U.; Wu, H. A.; Geim, A. K.; Grigorieva, I. V. Square Ice in Graphene Nanocapillaries. *Nature* **2015**, *519*, 443−445.

(5) Israelachvili, J. N.; McGuiggan, P. M.; Homola, A. M. Dynamic Properties of Molecularly Thin Liquid Films. *Science* **1988**, *240*, 189−191.

(6) Klein, J.; Kumacheva, E. Confinement-Induced Phase Transitions in Simple Liquids. *Science* **1995**, *269*, 816−819.

DOI: 10.1021/acs.jpcc.9b04839
J. Phys. Chem. C 2019, 123, 16902−16910

(7) Antognozzi, M.; Humphris, A. D. L.; Miles, M. J. Observation of Molecular Layering in a Confined Water Film and Study of the Layers Viscoelastic Properties. *Appl. Phys. Lett.* **2001**, *78*, 300−302.
(8) Raviv, U.; Laurat, P.; Klein, J. Fluidity of Water Confined to Subnanometre Films. *Nature* **2001**, *413*, 51−54.
(9) Zangi, R.; Mark, A. E. Bilayer Ice and Alternate Liquid Phases of Confined Water. *J. Chem. Phys.* **2003**, *119*, 1694−1700.
(10) Zangi, R. Water Confined to a Slab Geometry: A Review of Recent Computer Simulation Studies. *J. Phys.: Condens. Matter* **2004**, *16*, S5371−S5388.
(11) Knobler, C. M.; Desai, R. C. Phase Transitions in Monolayers. *Annu. Rev. Phys. Chem.* **1992**, *43*, 207−236.
(12) Tanaka, K.; Seto, T.; Hayashida, T. Phase Transformation of n-Higher Alcohols. (I). *Bull. Inst. Chem. Res., Kyoto Univ.* **1958**, *35*, 123−139.
(13) Tanaka, K.; Seto, T.; Watanabe, A.; Hayashida, T. Phase Transformation of n-Higher Alcohols. (II). *Bull. Inst. Chem. Res., Kyoto Univ.* **1959**, *37*, 281−293.
(14) Ramírez-Cardona, M.; Ventolà, L.; Calvet, T.; Cuevas-Diarte, M. A.; Rius, J.; Amigó, J. M.; Reventós, M. M. Crystal Structure Determination of 1-Pentanol from Low-Temperature Powder Diffraction Data by Patterson Search Methods. *Powder Diffr.* **2005**, *20*, 311−315.
(15) Shallard-Brown, H. A.; Watkin, D. J.; Cowley, A. R. *n*-Octanol. *Acta Crystallogr., Sect. E: Struct. Rep. Online* **2005**, *61*, o213−o214.
(16) Derollez, P.; Hédoux, A.; Guinet, Y.; Danède, F.; Paccou, L. Structure determination of the crystalline phase ofn-butanol by powder X-ray diffraction and study of intermolecular associations by Raman spectroscopy. *Acta Crystallogr., Sect. B: Struct. Sci., Cryst. Eng. Mater.* **2013**, *69*, 195−202.
(17) Böhmer, R.; Gainaru, C.; Richert, R. Structure and dynamics of monohydroxy alcohols-Milestones towards their microscopic understanding, 100 years after Debye. *Phys. Rep.* **2014**, *545*, 125−195.
(18) Oster, G.; Kirkwood, J. G. The Influence of Hindered Molecular Rotation on the Dielectric Constants of Water, Alcohols, and Other Polar Liquids. *J. Chem. Phys.* **1943**, *11*, 175−178.
(19) MacCallum, J. L.; Tieleman, D. P. Structures of Neat and Hydrated 1-Octanol from Computer Simulations. *J. Am. Chem. Soc.* **2002**, *124*, 15085−15093.
(20) Dannhauser, W. Dielectric Study of Intermolecular Association in Isomeric Octyl Alcohols. *J. Chem. Phys.* **1968**, *48*, 1911−1917.
(21) Fleshman, A. M.; Forsythe, G. E.; Petrowsky, M.; Frech, R. Describing Temperature-Dependent Self-Diffusion Coefficients and Fluidity of 1- and 3-Alcohols with the Compensated Arrhenius Formalism. *J. Phys. Chem. B* **2016**, *120*, 9959−9968.
(22) Morishige, K.; Kawano, K. Freezing and Melting of Methanol in a Single Cylindrical Pore: Dynamical Supercooling and Vitrification of Methanol. *J. Chem. Phys.* **2000**, *112*, 11023−11029.
(23) Morineau, D.; Guégan, R.; Xia, Y.; Alba-Simionesco, C. Structure of Liquid and Glassy Methanol Confined in Cylindrical Pores. *J. Chem. Phys.* **2004**, *121*, 1466−1473.
(24) Takamuku, T.; Maruyama, H.; Kittaka, S.; Takahara, S.; Yamaguchi, T. Structure of Methanol Confined in MCM-41 Investigated by Large-Angle X-ray Scattering Technique. *J. Phys. Chem. B* **2005**, *109*, 892−899.
(25) Morishige, K.; Mikawa, K. Tensile Effect on Crystal Nucleation of Methanol and Ethanol Confined in Pores. *J. Phys. Chem. C* **2012**, *116*, 3618−3622.
(26) Bampoulis, P.; Witteveen, J. P.; Kooij, E. S.; Lohse, D.; Poelsema, B.; Zandvliet, H. J. W. Structure and Dynamics of Confined Alcohol-Water Mixtures. *ACS Nano* **2016**, *10*, 6762−6768.
(27) Morishige, K.; Kawamura, K.; Kose, A. X-ray diffraction study of the structure of a monolayer methanol film adsorbed on graphite. *J. Chem. Phys.* **1990**, *93*, 5267−5270.
(28) Morishige, K. Structure and Melting of a Monolayer Ethanol Film on Graphite. *J. Chem. Phys.* **1992**, *97*, 2084−2089.
(29) Morishige, K.; Takami, Y.; Yokota, Y. Structures of Alkanes and Alkanols Adsorbed on Graphite in Solution: Comparison with Scanning-Tunneling-Microscopy Images. *Phys. Rev. B* **1993**, *48*, 8277−8281.
(30) Morishige, K. n-propanol on graphite: The occurrence of two-dimensional smectic mesophase. *J. Chem. Phys.* **1994**, *100*, 3252−3257.
(31) Morishige, K.; Sakamoto, Y. Melting of n-butanol and n-pentanol monolayers adsorbed on graphite: Effect of molecular length on melting. *J. Chem. Phys.* **1995**, *103*, 2354−2360.
(32) Morishige, K.; Kato, T. Chain-Length Dependence of Melting of n-Alcohol Monolayers Adsorbed on Graphite: n-Hexanol, n-Heptanol, n-Octanol, and n-Nonanol. *J. Chem. Phys.* **1999**, *111*, 7095−7102.
(33) Wolff, M.; Kruchten, F.; Huber, P.; Knorr, K.; Volkmann, U. G. Transition from van der Waals to H Bond Dominated Interaction in n-Propanol Physisorbed on Graphite. *Phys. Rev. Lett.* **2011**, *106*, 156103.
(34) Poirier, G. E.; Pylant, E. D. The Self-Assembly Mechanism of Alkanethiols on Au(111). *Science* **1996**, *272*, 1145−1148.
(35) Yang, T.; Berber, S.; Liu, J.-F.; Miller, G. P.; Tománek, D. Self-Assembly of Long Chain Alkanes and their Derivatives on Graphite. *J. Chem. Phys.* **2008**, *128*, 124709.
(36) Herwig, K. W.; Trouw, F. R. Ethanol on Graphite: The Influence of Hydrogen Bonding on Surface Melting. *Phys. Rev. Lett.* **1992**, *69*, 89−92.
(37) Morishige, K.; Hayashi, K.; Izawa, K.; Ohfuzi, I.; Okuda, Y. Formation of a bimolecular first layer intert-butanol on graphite. *Phys. Rev. Lett.* **1992**, *68*, 2196−2199.
(38) Morishige, K.; Kobayashi, N. Two-step melting of 2-propanol adsorbed on graphite. *J. Chem. Phys.* **1994**, *101*, 5209−5212.
(39) Zangi, R.; Roccatano, D. Strings-to-Rings Transition and Antiparallel Dipole Alignment in Two-Dimensional Methanols. *Nano Lett.* **2016**, *16*, 3142−3147.
(40) Hess, B.; Kutzner, C.; van der Spoel, D.; Lindahl, E. GROMACS 4: Algorithms for Highly Efficient, Load-Balanced, and Scalable Molecular Simulation. *J. Chem. Theory Comput.* **2008**, *4*, 435−447.
(41) Bussi, G.; Donadio, D.; Parrinello, M. Canonical Sampling through Velocity Rescaling. *J. Chem. Phys.* **2007**, *126*, 014101.
(42) Darden, T.; York, D.; Pedersen, L. Particle mesh Ewald: An N·log(N) method for Ewald sums in large systems. *J. Chem. Phys.* **1993**, *98*, 10089−10092.
(43) Hess, B.; Bekker, H.; Berendsen, H. J. C.; Fraaije, J. G. E. M. LINCS: A Linear Constraint Solver for Molecular Simulations. *J. Comput. Chem.* **1997**, *18*, 1463−1472.
(44) Walther, J. H.; Jaffe, R.; Halicioglu, T.; Koumoutsakos, P. Carbon Nanotubes in Water: Structural Characteristics and Energetics. *J. Phys. Chem. B* **2001**, *105*, 9980−9987.
(45) Zangi, R. Refinement of the OPLSAA Force-Field for Liquid Alcohols. *ACS Omega* **2018**, *3*, 18089−18099.
(46) Jorgensen, W. L.; Maxwell, D. S.; Tirado-Rives, J. Development and Testing of the OPLS All-Atom Force Field on Conformational Energetics and Properties of Organic Liquids. *J. Am. Chem. Soc.* **1996**, *118*, 11225−11236.
(47) Siu, S. W. I.; Pluhackova, K.; Böckmann, R. A. Optimization of the OPLS-AA Force Field for Long Hydrocarbons. *J. Chem. Theory Comput.* **2012**, *8*, 1459−1470.
(48) Ohno, K.; Yoshida, H.; Watanabe, H.; Fujita, T.; Matsuura, H. Conformational Study of 1-Butanol by the Combined Use of Vibrational Spectroscopy and ab Initio Molecular Orbital Calculations. *J. Phys. Chem.* **1994**, *98*, 6924−6930.
(49) Solomons, G.; Fryhle, C. *Organic Chemistry*; John Wiley & Sons, Inc.: New York, NY, 2002.

DOI: 10.1021/acs.jpcc.9b04839
J. Phys. Chem. C 2019, 123, 16902−16910

Supplementary Information: Self-Assembly of Alcohols Adsorbed on Graphene

Ronen Zangi*[1,2]

[1] *POLYMAT & Department of Organic Chemistry I, University of the Basque Country UPV/EHU, Avenida de Tolosa 72, 20018, San Sebastian, Spain*

[2] *IKERBASQUE, Basque Foundation for Science, Maria Diaz de Haro 3, 48013 Bilbao, Spain*

June 20, 2019

*Email: r.zangi@ikerbasque.org

a 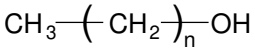

b 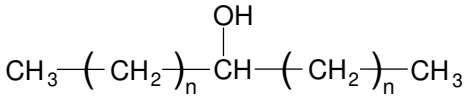

Figure S1: The alcohol molecules considered in this study. (a) The series of primary mono n-alcohols from ethanol (n=1) to 1-decanol (n=9), and (b) the symmetric secondary mono alcohols, 2-propanol (n=0), 3-pentanol (n=1), and 4-heptanol (n=2).

Table S1: Details of the setups of the series of simulations targeting adsorption at T=300 K for primary mono n-alcohols. The number of alcohol molecules, N, duration of the simulation time, t, and the temperature, T, are reported. The two-dimensional density, ρ_{2D}, of the last frame is also reported.

alcohol	(N, t [ns], T [K])	ρ_{2D} [kg/(mol·nm^2)]
1-butanol	(945, 6, 200) → (945, 13, 300) → (950, 20, 300) → (944, 20, 300) → (951, 20, 300) → (955, 20, 300) → (952, 100, 300)	0.218
1-pentanol	(777, 6, 200) → (777, 12, 300) → (782, 20, 300) → (787, 20, 300) → (784, 40, 300) → (782, 20, 300) → (781, 40, 300) → (781, 16, 320) → (780, 132, 300)	0.212
1-hexanol	(660, 6, 200) → (660, 18, 300) → (666, 20, 300) → (678, 20, 300) → (676, 20, 300) → (676, 40, 320) → (688, 20, 320) → (688, 20, 330) → (692, 20, 320) → (694, 38, 310) → (694, 60, 300)	0.219
1-heptanol	(600, 6, 200) → (660, 40, 300) → (604, 20, 300) → (604, 157, 320) → (603, 60, 340) → (600, 40, 330) → (600, 60, 310) → (608, 140, 310) → (612, 40, 310) → (610, 36, 300) → (614, 40, 300) → (612, 80, 300)	0.219
1-octanol	(560, 6, 200) → (560, 20, 300) → (544, 40, 300) → (544, 20, 350) → (543, 56, 350) → (552, 18, 350) → (558, 36, 310) → (558, 60, 300)	0.224
1-nonanol	(468, 6, 200) → (468, 12, 300) → (467, 20, 400) → (467, 38, 300) → (467, 20, 350) → (467, 38, 330) → (467, 218, 340) → (474, 40, 340) → (474, 40, 300) → (478, 100, 300)	0.213
1-decanol	(432, 6, 200) → (432, 20, 300) → (432, 20, 400) → (432, 20, 300) → (444, 20, 300) → (444, 278, 350) → (444, 60, 360) → (444, 60, 370) → (444, 40, 340) → (469, 80, 340) → (479, 30, 340) → (476, 120, 300)	0.232

Table S2: Details of the setups of the series of simulations targeting adsorption at T=250 K for ethanol and 1-propanol, as well as for the secondary alcohols, 2-propanol, 3-pentanol, and 4-heptanol. The number of alcohol molecules, N, duration of the simulation time, t, and the temperature, T, are reported. The two-dimensional density, ρ_{2D}, of the last frame is also reported.

alcohol	(N, t [ns], T [K])	ρ_{2D} [kg/(mol·nm^2)]
ethanol	(1386, 6, 200) → (1420, 20, 250) → (1439, 20, 250) → (1452, 20, 250) → (1451, 20, 250) → (1448, 20, 250) → (1446, 40, 250) → (1453, 80, 250) → (1462, 40, 250) → (1466, 72, 250) → (1465, 80, 250) → (1460, 80, 250) → (1459, 76, 250) → (1457, 100, 250) → (1455, 80, 250) → (1452, 80, 250) → (1451, 80, 250)	0.206
1-propanol	(1107, 6, 200) → (1107, 12, 300) → (1141, 215 250) → (1140, 40, 250) → (1139, 20, 250) → (1138, 40, 250) → (1137, 80, 250) → (1136, 80, 250)	0.211
2-propanol	(1080, 18, 200) → (1129, 20, 250) → (1198, 80, 250) → (1196, 40, 250) → (1195, 80, 250) → (1193, 100, 250) → (1190, 140, 250)	0.221
3-pentanol	(726, 20, 300) → (762, 20, 300) → (786, 20, 300) → (786, 152, 250)	0.214
4-heptanol	(630, 18, 300) → (627, 20, 300) → (627, 160, 250) → (624, 100, 250)	0.224

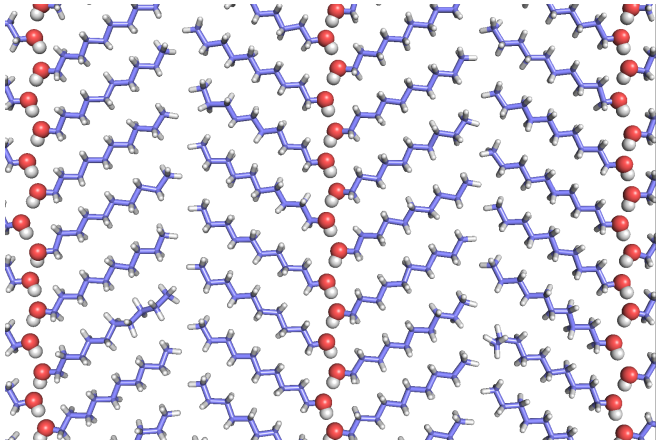

Figure S2: Magnification of the snapshot of 1-decanol shown in Fig. 2 depicting the zigzag pattern of the hydrogen bonds between the hydroxyl groups. The hydroxyl groups are represented by spheres wheres the tails by sticks.

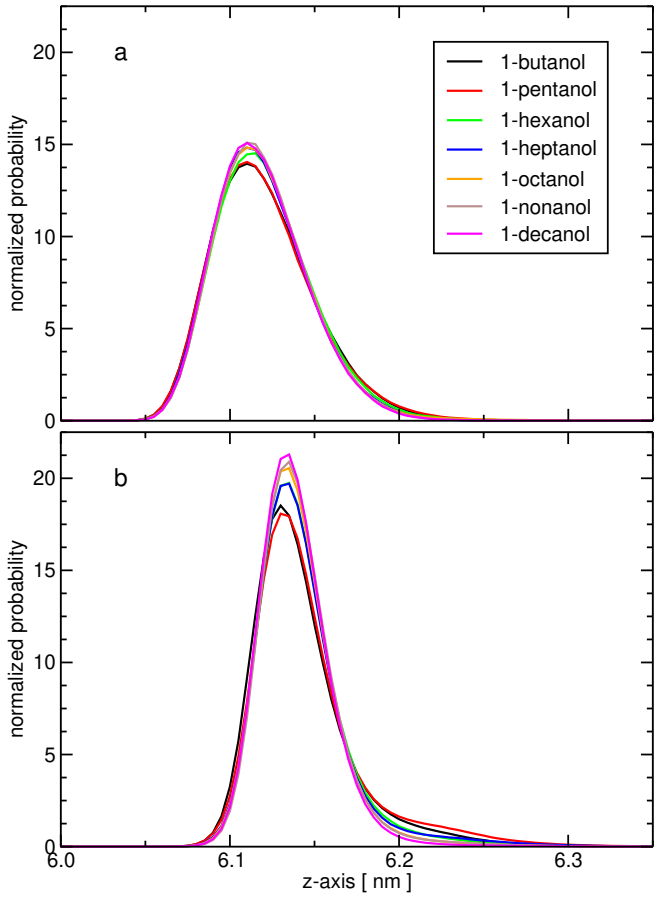

Figure S3: Normalized density profiles along the normal to the plane of the graphene sheet considering (a) the oxygen atoms, and (b) the carbon atoms of the adsorbed 1-alcohols at 300 K.

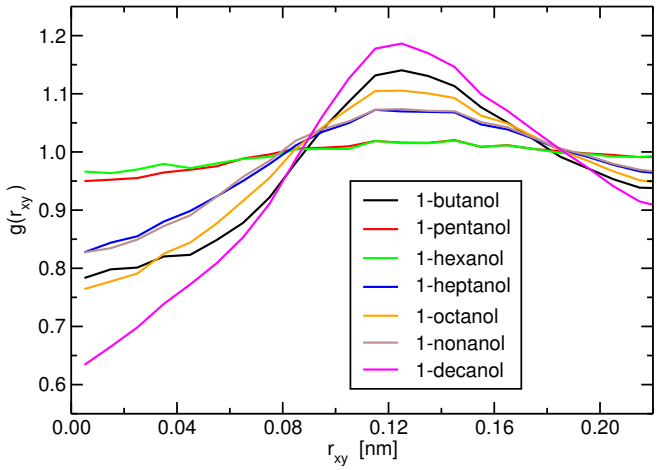

Figure S4: Two-dimensional radial distribution functions (in the *xy*-plane) between the carbon atoms of the alcohol tails and the atoms of the graphene sheet.

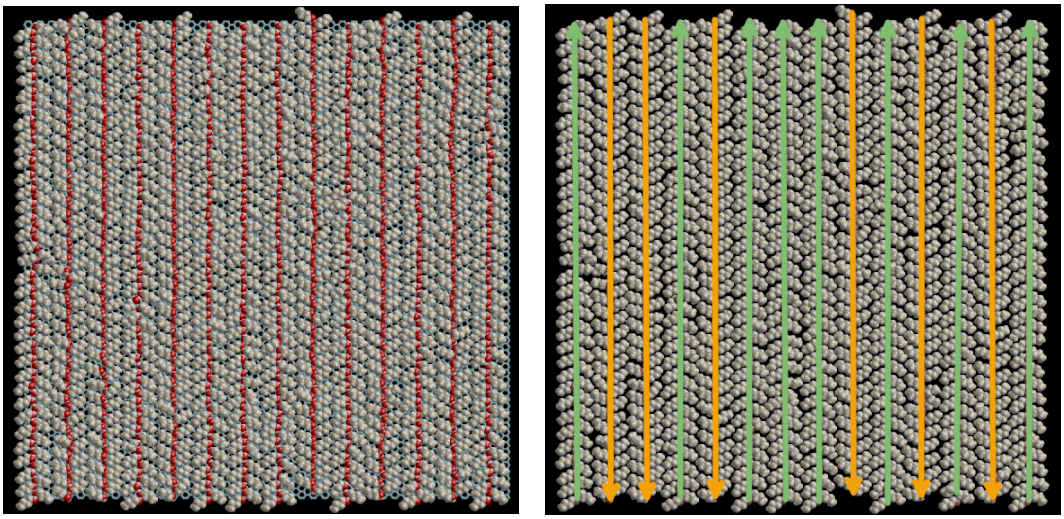

Figure S5: Left panel: The last configuration of 1-butanol adsorbed on graphene at 300 K shown in Fig. 1. Right panel: Same configuration but with arrows, placed on top of the hydrogen-bonded strings, pointing in the direction of Donor–H···Acceptor hydrogen-bond dipoles. Arrows colored in green and orange denote hydrogen-bond directions pointing up and down, respectively. In the right panel, the stick representation of the graphene sheet is not shown.

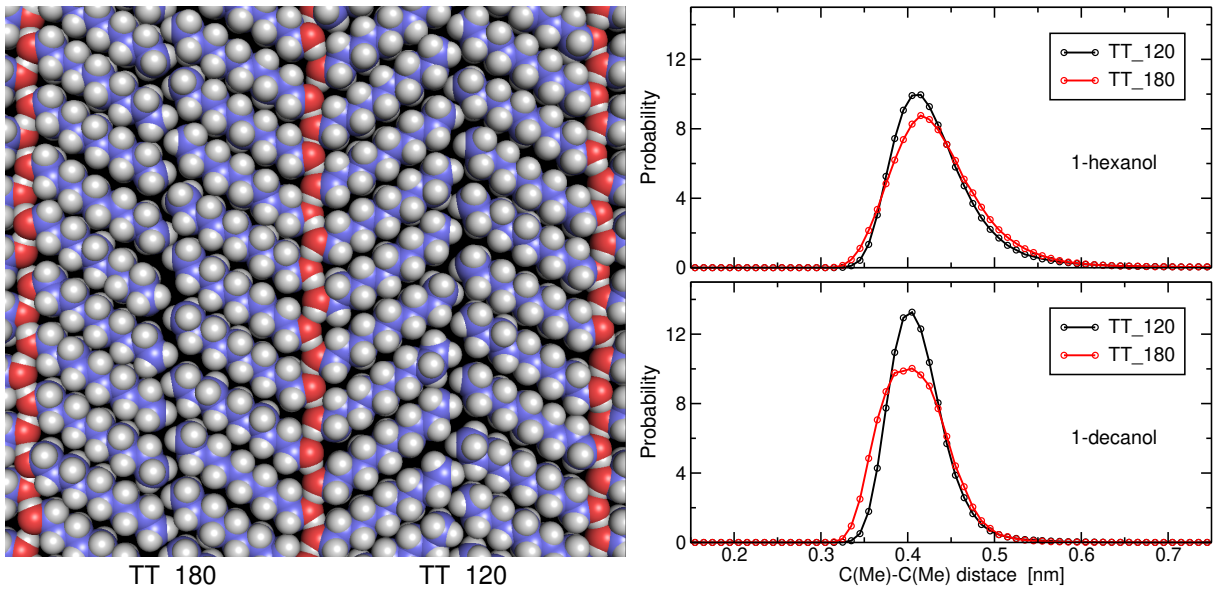

Figure S6: Left panel: A snapshot of 1-decanol taken from Fig. 2 displaying a central chain of alcohols that form with an adjacent chain on the left tail–tail interactions at 180 ° (TT_180), and with an adjacent chain on the right tail–tail interactions at 120 ° (TT_120). Right panel: Normalized distributions of the two-shortest methyl–methyl distances between different chains for the two patterns of tail–tail packings in 1-hexanol and 1-decanol.